

Mechanics of Advanced Materials and Structures

ISSN: (Print) (Online) Journal homepage: www.tandfonline.com/journals/umcm20

Improving piezoelectric energy harvesting performance through mechanical stiffness matching

Polat Kurt, Bastola Narayan, James I. Roscow & Sadettin Orhan

To cite this article: Polat Kurt, Bastola Narayan, James I. Roscow & Sadettin Orhan (25 Dec 2023): Improving piezoelectric energy harvesting performance through mechanical stiffness matching, Mechanics of Advanced Materials and Structures, DOI: 10.1080/15376494.2023.2295383

To link to this article: https://doi.org/10.1080/15376494.2023.2295383

© 2023 The Author(s). Published with license by Taylor & Francis Group, LLC

View supplementary material

Published online: 25 Dec 2023.

Submit your article to this journal

Article views: 502

View related articles

View Crossmark data

Full Terms & Conditions of access and use can be found at https://www.tandfonline.com/action/journalInformation?journalCode=umcm20

MECHANICS OF ADVANCED MATERIALS AND STRUCTURES
https://doi.org/10.1080/15376494.2023.2295383

Taylor & Francis
Taylor & Francis Group

ORIGINAL ARTICLE

OPEN ACCESS Check for updates

Improving piezoelectric energy harvesting performance through mechanical stiffness matching

Polat Kurt[a,b], Bastola Narayan[b], James I. Roscow[b], and Sadettin Orhan[a]

[a]Department of Mechanical Engineering, Ankara Yıldırım Beyazıt University, Ankara, Turkey; [b]Department of Mechanical Engineering, University of Bath, Bath, UK

ABSTRACT

The mechanical energy transfer between the source structure and active material in piezoelectric energy harvesters is investigated here. First, an analytical prediction to improve mechanical energy transfer into the piezoelectric material is proposed and validated by tailoring the stiffness of the beam to off-the-shelf piezocomposites through numerical models and experiments. An experimental study is then presented whereby the mechanical properties of freeze cast piezocomposites are controlled by adjusting the volume fraction of piezoceramic and epoxy filler phases. This offers a new approach for tailoring the mechanical properties of piezocomposites to maximize mechanical energy transfer into the material *via* stiffness matching.

ARTICLE HISTORY
Received 5 May 2023
Accepted 12 December 2023

KEYWORDS
Energy harvesting; piezoelectric; energy transfer; stiffness matching; freeze casting

1. Introduction

Piezoelectric energy harvesting has been widely studied in recent years as a method to convert otherwise dissipated mechanical energy into useful electrical energy [1, 2]. Typical harvested powers, however, remain in the micro- to milli-Watt range, and further effort is therefore required to boost these values toward a more useful magnitude. Piezoelectric energy harvesting systems are often formed by bonding the active piezoelectric materials to the mechanical source structure, such as a cantilever beam attached to a larger vibrating system designed to transfer the mechanical energy of the structure to the piezoelectric material. Here, many parameters, such as the piezoelectric and dielectric properties of the active material, the magnitude of the strain applied, its frequency, and the properties of the adhesive material affect the amount of electrical energy produced. The energy transfer between components within an energy harvesting system is a critical factor for maximizing the harvested electrical energy [3].

Piezoelectric energy harvesting from vibrating beams consists of four phases of energy transfer. Firstly, mechanical energy from the environment or a mechanical source is exerted on the host structure. This energy is converted to strain and kinetic energy, with some of the energy dissipated due to the mechanical damping of the beam. The strain energy in the beam is transferred to the piezoelectric material with some losses because of the unmatched mechanical impedance and stiffness between the two materials. Then, the strain energy in the piezoelectric material is converted to the electrical energy with an efficiency that is defined as the coupling factor, again with some conversion losses. Finally, the stored electrical energy is harvested using an external circuit. There is another potential loss in this step arising from unmatched electrical impedances between piezoelectric material and external circuit [4]. The energy flow for piezoelectric energy harvesting can be seen in Figure 1.

There have been many studies related to methods for improving harvested power from piezoelectric materials under vibration in recent years. Designing the beam structure to improve energy is one of the most influential methods. For example, Dawei et al. [5] designed a novel hybrid tri-stable energy harvester that improved the efficiency of power harvesting from piezoelectric materials. Ravanbod and Nejad [6] studied a meta-structure booster for energy harvesters and increased the generated power by nearly 15 times compared to a standard harvester with plain beam. A hexachiral auxetic structure with a negative Poisson's ratio was used by Shaik et al [7] to increase low-frequency power harvesting. It was found that using a hexachiral geometry increased the power response by 20 times compared to that of a plain beam. Silveira and Daniel [8] assembled a piezoelectric energy harvester to a tilting pad journal bearing to harvest energy. They have performed an optimization study based on the geometry and number of harvesters to be assembled and obtained an improvement of 35% in the harvested energy. Bouhedma et al. [9] presented a multi-resonant vibration harvester for ultra-low power applications and made a design optimization on the geometry of the harvester reaching a power density of

CONTACT James I. Roscow jir24@bath.ac.uk Department of Mechanical Engineering, University of Bath, Bath, UK.
Supplemental data for this article can be accessed online at https://doi.org/10.1080/15376494.2023.2295383

© 2023 The Author(s). Published with license by Taylor & Francis Group, LLC
This is an Open Access article distributed under the terms of the Creative Commons Attribution License (http://creativecommons.org/licenses/by/4.0/), which permits unrestricted use, distribution, and reproduction in any medium, provided the original work is properly cited. The terms on which this article has been published allow the posting of the Accepted Manuscript in a repository by the author(s) or with their consent.

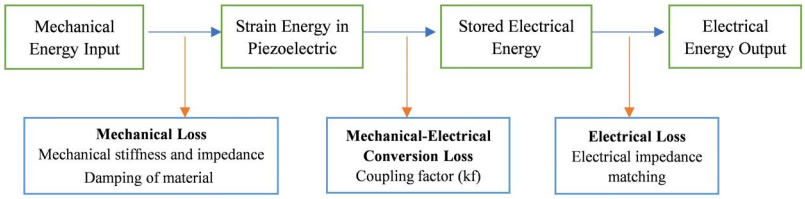

Figure 1. Energy flow of piezoelectric energy harvesting.

492 μW/cm^2. Chadha et al. [10] performed a comparative study including an auxetic core and found out that power output can be increased by 1.5 times compared to the conventional shapes with a reduction in weight of nearly 22%. Han et al. [11] studied seesaw-like structures for low-frequency vibration. It was found that the efficiency of the harvester depends on the moment of inertia and excitation frequency, and the harvester was found to have superior performance for low frequency and lower energy inputs. Askari et al. [12] investigated a multi-beam smart structure that offered a wide resonance frequency range that could be easily altered to match with the target application. They derived an analytical solution and compared the results with numerical simulation using COMSOL Multiphysics. A non-uniform beam structure was studied by Raju et al. [13] using rectangular and tapered shapes containing cavities. They used mathematical modeling alongside experimental verification and demonstrated a 90% increase in output energy compared to the uniform structure.

Furthermore, tuning the mechanical and electrical impedances of materials is important to maximize energy transfer. Electrical impedance matching between the piezoelectric material and electrical circuit to increase the harvested energy has been studied intensively in the literature [14]. The maximum power transfer from the piezoelectric material can be obtained if the external load impedance is the complex conjugate of the material's impedance. However, it may be unpractical to use the complex conjugate impedance directly because of the need for a large inductor. Na et al. [15] presented resistive impedance matching to overcome this and around 58–72% of the maximum available stored energy was harvested by this method. Another method was suggested by Hamid et al. [16] in which they reported the efficiency being around 60% in the stage of conversion of stored electrical energy to harvested electrical energy. Bao and Junrui [17] introduced an impedance-based model using different circuits and it was verified by simulation and experimental results. An electrical impedance matching study was performed by Michele et al. [18] aiming to maximize the power response at a desired frequency. A 3-fold power increase in a wide frequency range was achieved.

The energy flow and energy conversion efficiency for the complete harvesting process have been investigated by several researchers. Yang et al. [19] analyzed the energy flow between applied mechanical energy and harvested electrical energy based on a single degree of freedom (SDOF) model. They derived an expression for energy flow for linear cantilever energy harvesters and validated it experimentally. The efficiency of a piezoelectric energy harvesting system was also analyzed by Kim et al. [20]. Instead of optimizing the power output, it was suggested to use the efficiency optimization for a fair comparison of energy harvesting systems with different parameters, such as geometry, size, operating conditions, etc. For rectified piezoelectric power harvesters, an analytical model was established by Shu and Lien [21] where the efficiency for the conversion of the energy of the harvester was shown to depend on the electrical resistance, frequency ratio, electromechanical coupling coefficient, and damping ratio. Uchino [22, 23] has widely investigated the steps of the energy transfer of piezoelectric energy harvesters individually. He stated the importance of mechanical energy flow from the substructure to the piezoelectric material using the mechanical impedance matching theory. He also suggested the importance of considering the mechanical rigidity of the materials by implementing an experiment for the energy flow of a cymbal transducer with changing thickness.

The literature studies on energy harvesting and energy transfer efficiency are generally focused on the whole energy transfer process or electrical impedance matching, as discussed above. Mechanical energy transfer and mechanical impedance matching were investigated by Uchino [23] on a cymbal transducer that was working under an impact force. However, there is a lack in the literature focussed on tailoring the mechanical energy transfer of vibration energy harvesters and the effect of the mechanical stiffnesses of the active piezoelectric material on the overall energy transfer efficiency.

The effective stiffnesses of the materials should be considered in energy harvesting applications to increase the power output. For example, bonding a high-stiffness piezoelectric material, such as PZT ($Y = 60$GPa) onto an acrylic ($Y = 3.2$GPa) beam with a significantly lower stiffness results in poor harvesting performance as much of the mechanical energy in the beam cannot be transferred to the piezoelectric. In this scenario, increasing the effective stiffness of the structure onto which the piezoelectric element is bonded would be one way to improve the harvester output. Modifying the base structure has previously been shown to improve the energy transfer into the piezoelectric material [24]. However, in some cases, the substructure cannot be modified as its properties may be defined by other functional factors, and the piezoelectric material should be the one to be mechanically altered to match its working environment. Whilst the mechanical properties of piezoelectric ceramics and single crystals cannot be easily tailored, composites offer a method of controlling both mechanical and functional properties [4]. Therefore, they can be used to manage the impedance matching in energy harvesting applications but most research into piezoelectric composites for energy harvesting has focussed on maximizing the figure of

merit, $d_{ij}^2/\varepsilon_{33}^T$, where d_{33} is the piezoelectric charge coefficient and ε_{33}^T is the constant stress permittivity, rather than investigating the benefits of tailoring their mechanical properties.

The most common piezoelectric composites are produced by the dice-and-fill method whereby dense piezoelectric materials are sectioned and the spaces filled with epoxy [25]. By sectioning the monolithic ceramics or single crystals into thin sections ($\sim$300 μm) and encapsulating in a polymer a degree of flexibility and damage resistance can be achieved, which is important for cantilever-based energy harvesters, hence the widespread use of Macro-Fiber Composites^{TM} (MFCs) produced by Smart Material Corp. in the energy harvesting literature [24, 26, 27]. This method requires expensive machining equipment, and as such piezoelectric composites based on porous piezoceramics have gained attention in recent years. They can be produced with desired pore structure and infiltrated with polymers to improve mechanical properties. The freeze casting technique, for example, can produce highly aligned porous piezoceramics with high energy harvesting figures of merit [28–30]. In the freeze casting method, a suspension of piezoelectric ceramic powder, a liquid medium (typically water), dispersant, and binder is prepared and then directionally frozen along a temperature gradient. As the liquid solidifies, crystallites grow along the temperature gradient and force the ceramic powder into aligned channels. After freezing is completed, the frozen liquid phase is sublimated to preserve the templated structure. The dispersant and binder are then removed through heat treatment, and the ceramic channels consolidate during the sintering process to leave a highly aligned porous piezoelectric ceramic. It has been shown that porous piezoceramics produced with this method offer high longitudinal piezoelectric charge coefficients, d_{33}, comparable with dense piezoceramics of the same material composition, and low constant stress permittivity, ε_{33}^T, which leads to high longitudinal piezoelectric voltage coefficients, $g_{33} = d_{33}/\varepsilon_{33}^T$ and high harvesting figure of merits, $d_{33}g_{33}$ compared to their dense counterparts [29]. The final volume fraction of ceramic, and therefore the mechanical properties, can be easily adjusted by controlling the solid loading within the initial suspension [31].

This paper aims to investigate the effect of the mechanical stiffness ratio between the active piezoelectric material and the structure on which it is bonded on the harvested energy. The second focus of the study is to offer a method to produce piezoelectric composites with high figures of merit and mechanical properties that can be easily adapted depending on the application. Firstly, the mechanical energy transfer into a commercial piezoelectric material patch is optimized by altering the mechanical properties of the beam. An equation to simply predict the mechanical energy transfer efficiency due to the stiffnesses of the materials is proposed and a study consisting of different piezoelectric materials bonded on metal beams with different effective stiffnesses was implemented to verify the results using finite element analysis and experimental work. The proposed equation only considers the effect of the mechanical stiffnesses of the materials on mechanical energy transfer and does not consider the other parameters that effect the harvested power from piezoelectric material, such as damping, electrical impedance matching, and electromechanical conversion ratio, etc., as they have already discussed widely in the literature. Secondly, piezoelectric composites with varying volume fractions of piezoceramic phase are formed *via* freeze casting to modify the mechanical properties of the piezocomposite rather than the substructure. The method proposed in this paper can be used as a guide in the materials selection process and piezocomposite design to maximize the mechanical energy transfer process of piezoelectric harvesters.

2. Method

2.1. Part 1: Enhancing energy harvesting performance by tailoring beam stiffness

2.1.1. Theory for increased energy transfer

Piezoelectric materials convert the strain energy into usable electrical energy. It is therefore important to maximize the strain energy exerted on the piezoelectric material to yield a high electrical energy output.

Considering a beam with bonded piezoelectric patches excited with a mechanical energy source as shown in Figure 2, the input mechanical energy can be written as follows [23]:

$$P_{in} = F\dot{w} \tag{1}$$

where F is the applied force or acceleration and w is the displacement change of force in z-direction. The strain energy in the beam and in piezoelectric patches is:

$$U_{strain} = \frac{1}{2}\int_0^l YI\left(\frac{d^2w(x,t)}{dx^2}\right)^2 dx \tag{2}$$

where Y is the modulus of elasticity of material, I is the area moment of inertia, and $w(x,t)$ is the response in z-direction. The electrical energy stored within the piezoelectric material, assuming it to behave as a parallel plate capacitor, can then be calculated as:

$$U_{elec} = \frac{1}{2}CV^2 \tag{3}$$

and the harvested power from the external circuit,

$$P_{out} = V^2/R \tag{4}$$

where C is the capacitance of the material, V is the piezoelectric voltage response and R is the external resistance.

As shown in Figure 1, there are three steps of the energy transfer in piezoelectric energy harvesting. The first step is the energy transfer from the external energy source to the harvester. When the force is applied to the tip in Figure 2, some of the energy is stored in the substructure and some of the energy is dissipated through damping. The stored

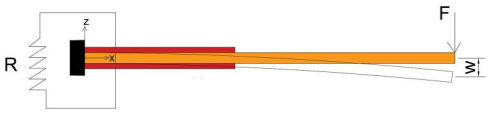

Figure 2. Piezoelectric energy harvesting by an external energy source.

mechanical energy is transferred to the piezoelectric material with some loss in the interface due to the mechanical impedance and stiffness matching [23]. The stored mechanical energy in the piezoelectric material is converted to the electrical energy with electromechanical coupling factor, k^2, which is given by [4],

$$k_{ij}^2 = \frac{\text{Stored electrical energy in piezoelectric}}{\text{Stored mechanical energy in piezoelectric}} = \frac{d_{ij}^2}{\varepsilon_{ii}^T s_{jj}^E} \tag{5}$$

where d_{ij} is the piezoelectric strain coefficient, s_{jj}^E is the mechanical compliance of the material under constant electric field conditions and ε_{ii}^T is the permittivity at constant stress. This stored electrical energy can be harvested using an external circuit, and the efficiency of this process is related to the electrical impedance matching. Therefore, the total efficiency of the harvesting process can be written as follows:

$$\begin{aligned}\text{Total Efficiency} = {} & (\text{Mechanical Transfer Efficiency}) * \\ & (\text{Piezoelectric Conversion Efficiency}) * \\ & (\text{Electrical Energy Transfer Efficiency})\end{aligned} \tag{6}$$

This can be calculated as follows:

$$\text{Total Efficiency} = \frac{P_{out}}{P_{in}} = \frac{V^2/R}{F\dot{w}} \tag{7}$$

In this study, off-resonance analysis was made with open-circuit conditions to eliminate the effects of the damping, frequency shift, and electrical impedance matching on the energy transfer efficiency. As such, we are able to focus on the mechanical impedance matching part of the energy transfer process. The electromechanical coupling coefficient has been kept constant using the same MFC material. Therefore, the total efficiency calculated with different conditions considers only the mechanical transfer efficiency:

$$\text{Total Efficiency} = (\text{Mechanical Transfer Efficiency}) * \left(k_{ij}^2\right) * (\text{EIM}) \tag{8}$$

where, EIM is the electrical impedance matching efficiency. In this efficiency term, the k_{ij}^2 and EIM terms remain constant and are omitted from the equation. Therefore, the change in total efficiency calculated based on Eq. (7) only relates to changes in the mechanical transfer efficiency.

Studies in the literature [19, 20] analyze the efficiency of the whole process in energy harvesting as defined in Eq. (7). However, the effect of stiffness mismatch or mechanical impedance mismatch in mechanical-mechanical energy transfer was not considered in these studies. Using Eq. (2), we can see that strain energy strongly depends on the effective stiffness (YI) of the material and structure. If the piezoelectric patch is too stiff compared to substructure the energy transfer will be low as the beam cannot bend sufficiently. On the other hand, if the substructure is too stiff compared to piezoelectric patch, a higher external mechanical energy will be required to deform the substructure, and therefore the piezoelectric patch, by the same distance. This implies there is an optimum for the energy transfer ratio between the piezoelectric material and beam to be maximized. Here, we offer a prediction for energy transfer efficiency from substructure to the piezoelectric material, based on the mechanical-mechanical energy transfer of Uchino [23],

$$\eta_{\text{mech-pred}} = 1 - \frac{(K_2 - K_1)^2}{(K_2 + K_1)^2} = 1 - \frac{(1 - K_1/K_2)^2}{(1 + K_1/K_2)^2} \tag{9}$$

where, K_1 and K_2 are the effective stiffnesses of the piezoelectric patch and the beam, and K_1/K_2 can be defined as an effective stiffness ratio. This equation enables us to predict the efficiency of the mechanical energy transfer from the substructure to the piezoelectric, which reaches a maximum when the effective stiffnesses of the piezoelectric patch and beam are equal. This is related to the effective stiffness of each of the piezoelectric and the beam, which is proportional to both the material properties (e.g. Young's modulus) and geometry (area moment of inertia) of the structures in the direction of applied force. The stiffnesses can be written as follows for transverse (in z-direction) vibrations:

$$K_1 = Y_p I_p, \;\; K_2 = Y_s I_s \tag{10}$$

where Y_p and Y_s are modulus of elasticities of the piezoelectric material and substructure in the direction of strain applied, respectively, and I_p and I_s are area moment of inertia of these materials. This equation is valid for cases where piezoelectric patch covers less area than the half of the substructure but becomes less reliable for increased coverage ratios of the piezoelectric patch to beam. It would need to be adapted for cases where the piezoelectric patch becomes more dominant to the overall structural stiffness as it approaches a full covering.

2.1.2. Finite element modeling

In this section, several analyses were implemented to investigate the effect of the mechanical stiffness of both beam and piezoelectric patch on the energy harvesting performance. COMSOL Multiphysics (v5.2a) finite element analysis software was used along with the SOLIDWORKS (v.2016) modeling software. For all the cases, cantilevered beams with piezoelectric materials bonded on both sides were modeled (bimorph configuration). Using symmetric configurations, such as bimorph harvesters locates the neutral axis in the middle of the structure, which simplifies the calculation of the stiffnesses of materials. If the neutral axis position does not lie centrally its position should first be calculated and then mechanical stiffnesses of the materials calculated based on this position.

First, a beam with a piezoelectric material bonded onto its surfaces was modeled in SOLIDWORKS. The model was then transferred to COMSOL using the Livelink Interface between two programmes. The dimensions of the modeled beam and piezoelectric patch are shown in Figure 3. The dimensions of the piezoelectric patches were kept constant in all cases to fix the mechanical stiffness of the patches. Rather, the thickness of substructure (t_s) is altered through the cases to change the mechanical stiffness of the substructure to investigate the effect of stiffness matching between the substructure and the

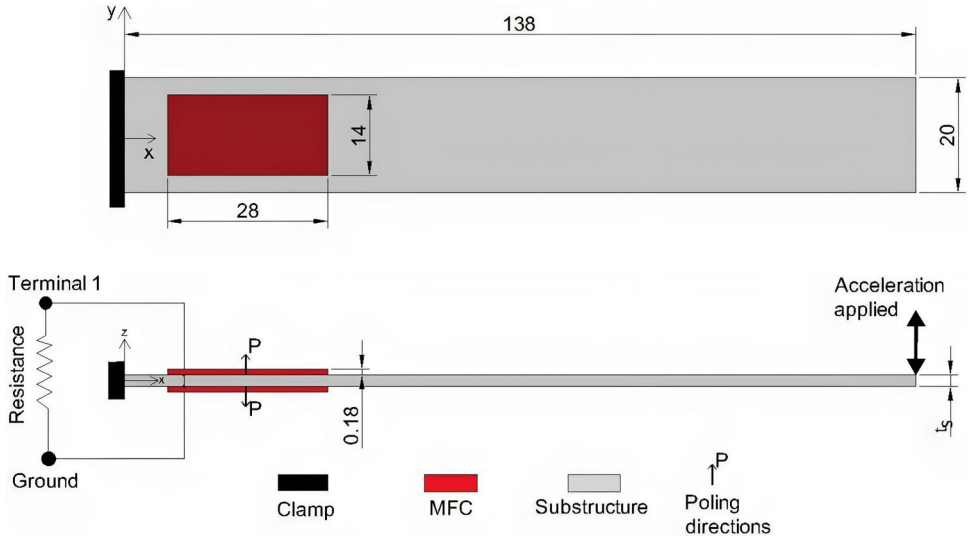

Figure 3. Dimensions of the modeled cantilever geometry. All units are in mm.

piezocomposite patch. Different piezoelectric materials were used in the analysis to see how the results varied by structure.

A 3D space environment was used in the analysis with piezoelectricity physics which includes solid mechanics and electrostatics interfaces. The beam and piezoelectric materials were assumed to be perfectly bonded to each other [32]. Frequency domain analysis was performed in a range of specified frequencies which are given later in the details of the studies. The multimode response of the beam was not investigated in this study. Rather the focus was to demonstrate the effect of mechanical energy transfer by comparing the results to the same type of harvesters by operating the beams in the first modal response. One end of the beam was fixed to give a clamped condition and an acceleration was applied to the other end in the Z-direction as shown in Figure 5. The substructure material was assigned as a linear elastic material. The two piezoelectric materials modeled on the substructure surface were poled in opposite directions for serial connection, with the poling direction controlled by rotating the coordinate axis by 180° in Z. Damping was not considered as the analysis was for off-resonance behavior of the structures. Furthermore, the aim of the analysis was to study the mechanical energy transfer efficiency rather than investigating power response levels near resonance. The modeled piezoelectric energy harvester was then connected to an external circuit with two terminals and one ground node added. The top of piezoelectric material 1 was assigned as terminal one and the bottom of piezoelectric material 2 was assigned as the ground node. The other two surfaces, i.e. the bottom of the top piezoelectric patch and the top of the bottom piezoelectric patch, were connected with the node of terminal two such that they were connected in series. A resistor and an external terminal were defined, with terminal one selected to measure the electric potential generated by the piezoelectric harvester. In the Multiphysics tab in COMSOL, piezoelectric effect was defined for piezoelectric materials. Finally, the structures were meshed using free tetrahedral and triangular elements. Using smaller mesh sizes increases the accuracy of the result but also increases the time for the model to solve. Therefore, a mesh convergence study was performed, and a total of 24,000 elements were found to give good accuracy with reasonable solving times. It was an average value and changed slightly according to the thickness of the beams used in the analysis. The voltage responses and the elastic strain energy applied to the beam of the piezoelectric materials were measured within COMSOL and the efficiency of the energy harvesting process was then calculated using Eq. (7).

Table 1. Material properties of the piezoelectric materials used in FEA model.

	MFC	PZT-5A	PVDF
Density (kg/m^3)	6757	7950	1780
Elasticity in x direction (GPa)	51	66	8.3
Relative permittivity, $\varepsilon_{33}^T/\varepsilon_0$	1867	1800	10
Piezoelectric charge constant—d_{31} (pC/N)	−171	−190	6
Dimensions (mm^3)	28 × 14 × 0.18	28 × 14 × 0.18	28 × 14 × 0.18

Table 2. Material properties of the substructure materials used in FEA model.

	Steel	Aluminum	Acrylic
Density (kg/m^3)	8000	2700	1180
Modulus of elasticity (GPa)	192	70	3.2
Poisson's ratio	0.31	0.33	0.35

In this part of the study, different piezoelectric materials [PZT-5A, PVDF (polyvinylidene fluoride), and MFC] were used with steel, aluminum, and acrylic substructures materials. These materials have different mechanical properties and are commonly used in the literature for energy harvesting applications. The required material properties of all materials except MFC were taken directly from the literature [33, 34] and are given in Tables 1 and 2. However, the properties of the MFC patches were not readily available and therefore had to be calculated. The MFCs consist of piezoelectric lead zirconate titanate (PZT) fibers which are aligned to the primary loading axis and encapsulated in epoxy. The volume fractions of PZT fibers and epoxy are $v_{PZT} = 0.85$ and $v_{epoxy} = 0.15$, respectively. The composite is electroded on top and bottom with copper fingers and encapsulated with a Kapton layer as shown in Figure 4. P2 type MFCs that work in d_{31} mode

were used in this study. The properties of MFCs have been modeled previously [35–37] but here a simpler model is used to define the MFC properties. The properties given in the MFC datasheets are for the encapsulated end-product, however, in this study, only the piezocomposite part of the MFC was modeled to simplify the process and the data were therefore adapted for this purpose. This approach agreed well with experimental data.

The material properties of MFC were defined with respect to the direction of the primary strain axis. The constant stress permittivity (ε_{33}^{T}) of the MFC was calculated from capacitance data which was measured using a Solartron SI 1260 and 1296 (Solartron Analytical, UK); Table 1 gives the relative permittivity $\varepsilon_{33}^{T}/\varepsilon_0$ where ε_0 is the permittivity of free space. The piezoelectric charge coefficient (d_{31}) was calculated from the average free strain per volt data taken from the manufacturer datasheet [38] and using the equation:

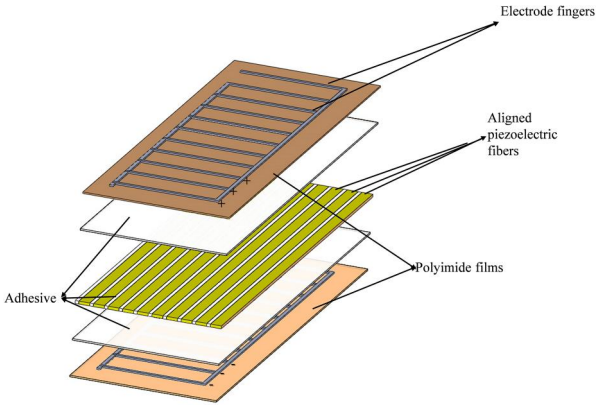

Figure 4. Exploded view of an MFC [23]. [With permission of Smart Material Corp.].

$$d_{31} = \frac{S_1}{V_3} t \tag{11}$$

The density, ρ_{MFC}, and the modulus of elasticity, Y_{MFC}, were calculated based on the piezoelectric fiber volume fraction ($v_{\mathrm{PZT}} = 0.85$; $v_{\mathrm{epoxy}} = 0.15$) of the MFC and linear mixing rules for the composites, where [39]:

$$\rho_{MFC} = v_{\mathrm{PZT}}(\rho_{PZT}) + v_{epoxy}(\rho_{epoxy}) \tag{12}$$

$$Y_{MFC} = v_{\mathrm{PZT}}(Y_{PZT}) + v_{epoxy}(Y_{epoxy}) \tag{13}$$

The modified material properties of MFC used in the finite element study are shown in Table 1.

2.1.3. Experimental validation

A piezoelectric energy harvesting setup was built to validate the model; a schematic is shown in Figure 5. First, steel beams ($w = 20$ mm, $l = 138$ mm) with different thicknesses ($t_s = 0.25$, 0.50, 0.70, and 1.15 mm) were cut from sheet metal. M2814-P2 type MFCs were bonded on each side of the beam in the same position (see Figure 6). One side of the beam was connected to the shaker and the other side was clamped. The shaker was connected to a function generator whose signal was passed through an amplifier. An acceleration sensor was placed on the shaker to measure the applied acceleration on the beam. The piezoelectric materials were connected to each other in series and then attached and connected to the resistance box to make an external circuit. A sinusoidal signal was generated by the function generator that was then amplified. The applied acceleration of the vibration shaker was measured by an acceleration sensor, and the amplification gain was adjusted so that this was the same for each test. The generated voltage from the piezoelectric and the acceleration signal were

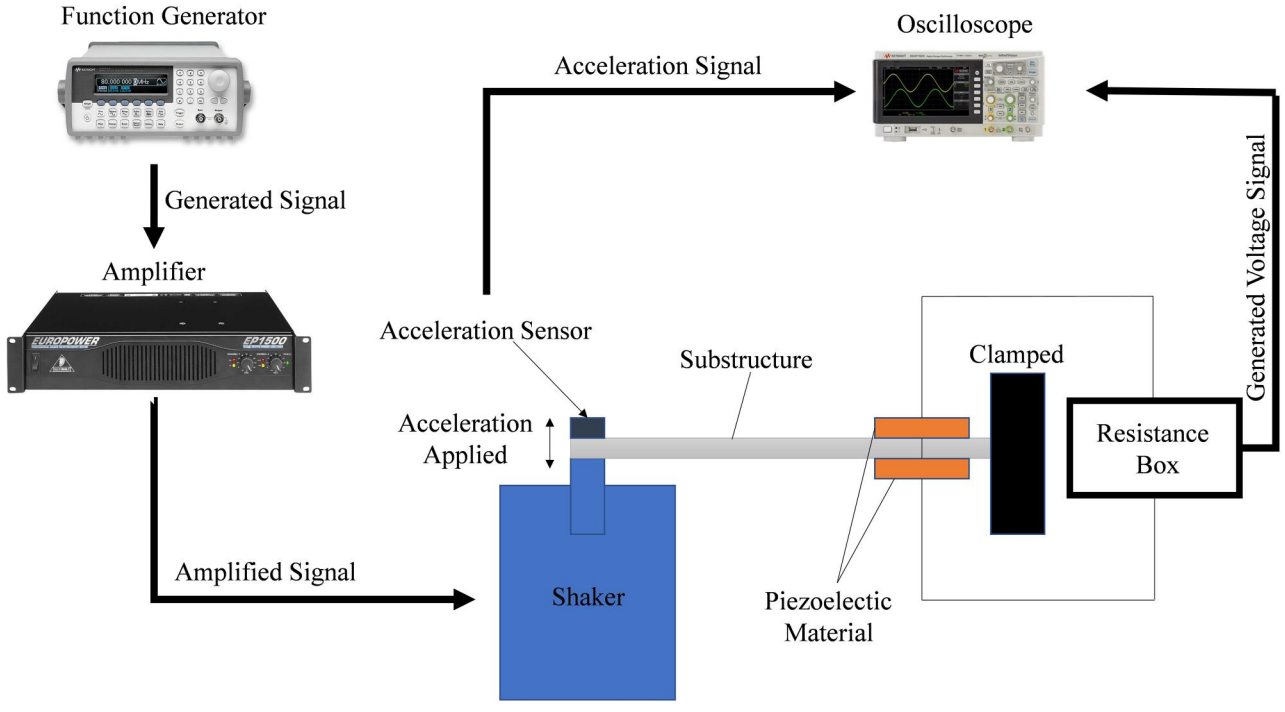

Figure 5. Schematic of energy harvesting experimental setup.

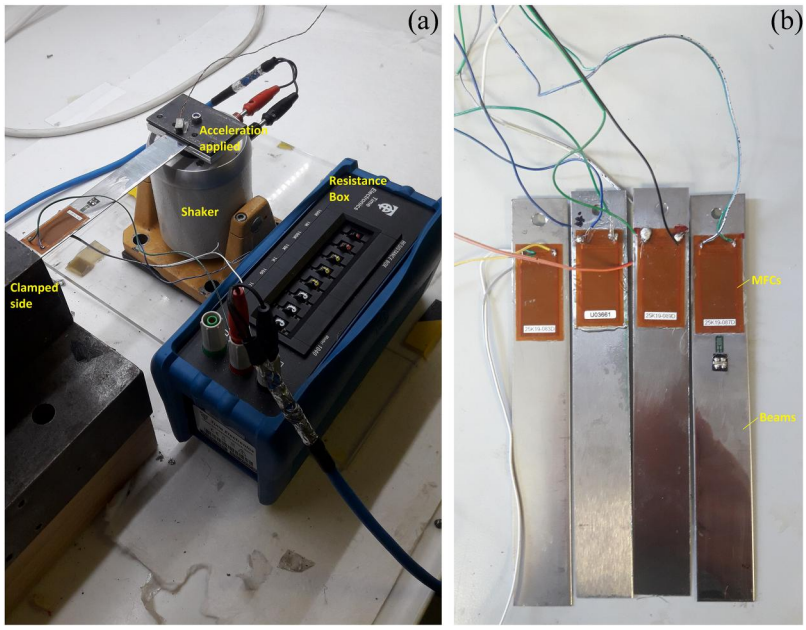

Figure 6. (a) Energy harvesting set-up with (b) MFCs bonded on the beams.

sent to the oscilloscope. The results were taken manually from the oscilloscope for each step by using peak to peak data. The voltage responses were calculated and normalized to the 1 g of acceleration based on the measured acceleration.

2.2. Part 2: Tailoring mechanical properties of freeze cast piezocomposites

2.2.1. Fabrication of piezocomposites

The first part of this study is intended to demonstrate how the structural properties of a harvesting system can be tailored to maximize the mechanical energy transfer into the piezoelectric material. In many circumstances, however, it is not possible to alter the properties of the system (e.g. the system tends to already be optimized for its primary application) and so it is beneficial to tailor the properties of the piezocomposite to the environment it is being used within. This is the case for piezoelectric materials used for underwater acoustic sensors, for example, whereby lowering the density and stiffness of the piezoelectric by forming a composite between a ceramic or single crystal and a polymer improves the acoustic impedance matching and therefore the performance of the sensor [14]. In this part of the study, we fabricated piezoelectric composites using the freeze casting method, which provided control over the volume fraction of piezoelectric composite.

The fabrication of the freeze cast piezoelectric composites consisted of two phases: (1) freeze casting of porous piezoelectric ceramics and (2) infiltration of epoxy into these pores. For the freeze casting process, commercially available PZT powder (NCE55, Noliac, Denmark) was ball milled in polyethylene containers with 2 mm diameter zirconia milling media and ethanol for 24 h to break up agglomerates formed during spray-drying. The powder was dried and sieved before being used to form the initial freeze casting suspensions. Suspensions were formed with different volumetric concentrations ratios of powder (30, 40 vol.%) to deionized water with 1 wt.% of polyethanol glycol (PEG, mw = 8000 g/mol, Sigma, UK) and 1 wt. % of ammonium polyacrylate dispersant (HydroDisper A160, Shenzhen Highrun Chemical Industry Co. Ltd, China) and suspensions were mixed on a ball mill for 24 h. These suspensions were then poured into a rectangular silicone mold with aluminum tape backing that was placed on a plate pre-cooled to a temperature of −70 °C using a low temperature circulation system (Lauda, RP2090, UK) and left until the suspensions were fully frozen. The top surface of the mold was maintained at room temperature to provide a temperature gradient across the mold to drive directional ice growth. Freezing rates were not measured directly; rather, the temperature of cold plate was maintained at a set value (−70 °C) throughout the freezing process. Only the temperature of the plate was measured throughout the process. The frozen bodies were then freeze dried for 24 h (Mini Lyotrap, LTE Scientific, UK) to remove ice from the bodies before sintering in closed alumina crucibles with around 3 g of sacrificial powder to compensate for lead loss. The samples were heated to 400 °C and maintained at that temperature for 2 h to remove organic additives, and then sintered at 1200 °C for 2 h; a heating rate of 1 °C/min was used. The furnace was then cooled at a rate of 2 °C/min to room temperature.

Two porous PZT samples with different porosities were fabricated in dimensions of $11 \times 11 \times 23\,mm^3$. See Figure 7 for a schematic of the freeze casting process. The sintered PZT samples were Corona poled with a 20 kV point source which was 35 mm from the base of the poling rig at 120 °C for 15 min and allowed to cool to 40 °C whilst the poling voltage was maintained. The poled samples were infiltrated with epoxy resin to form the piezoelectric composites with improved mechanical strength to the initially sintered porous PZT ceramics. As the epoxy was added after the porous piezoceramics were sintered it did not alter the pore

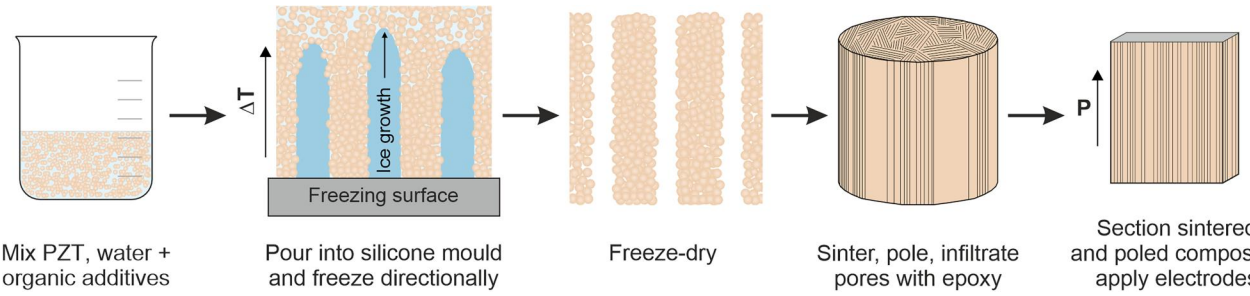

Figure 7. Freeze casting process to form porous piezoceramics. The sintered bodies were then sectioned and infiltrated with polymer to form the composites. Adapted from Ref. [33].

structure of the materials. The polarization direction is in the length direction of the samples as can be seen in Figure 7. Then, they were electroded with silver paint (RS Components, Product No 186-3600, UK) from the top and bottom of the material in the direction of polarization to operate in d_{33}-mode, allowed to dry at room temperature and sectioned to the $9 \times 1.4 \times 20\,\text{mm}^3$ dimensions using a diamond wire saw (STX-202A, MTI Corporation, USA).

2.2.2. Material characterization

The samples were weighed and measured before the infiltration process and the densities of the samples were calculated. The porosities of the samples were evaluated from the relative densities with respect to commercial the PZT, using the relationship:

$$v_{pore} = 1 - \frac{\rho_c}{\rho_{PZT}} \tag{14}$$

where v_{pore} is the volume fraction of porosity, ρ_c is the density of the piezoelectric composites which was calculated from their weight and volume of the material, and ρ_{PZT} is the density of the dense PZT ($8\,\text{g/cm}^3$). Scanning electron microscopy (SEM) was used to characterize the microstructures (Hitachi SU-3900, Japan). Freeze cast porous samples were infiltrated with epoxy resin (Araldite 2020 Liquid Adhesive, Huntsman International LLC, USA) and cut along the freezing direction before being attached to the sample holder using carbon tape. Images in backscatter mode were collected to understand the pore morphology and polymer infiltration. The electromechanical properties of the samples were measured after the infiltration process. Piezoelectric charge coefficients (d_{33}) were measured using a piezometer (Piezotest, PM300, Singapore) at a static load of 10 N and a dynamic load of ± 0.1 N applied at 97 Hz, with the output charge collected from electrodes perpendicular to the poling axis. Three repeat measurements were taken for each sample and the average was taken. Impedance spectroscopy was used to measure the dielectric properties and estimate the mechanical properties of the samples, using a Solartron SI 1260 and 1296 (Solartron Analytical, UK). An AC voltage of ± 0.1 V was applied to the sample and the generated current was measured from 1 MHz and 1 Hz. The unclamped (constant stress) permittivity of the samples was calculated from capacitance values measured from impedance data at 1 kHz, using the formula:

$$\varepsilon_{33}^{T} = \frac{Ct_c}{A\varepsilon_0} \tag{15}$$

where C is the capacitance of the material, t_c is the thickness of the composite and A is the area of the electrode. The piezoelectric voltage coefficient was calculated from the piezoelectric charge coefficient and permittivity:

$$g_{33} = \frac{d_{33}}{\varepsilon_{33}^{T}} \tag{16}$$

This was used to calculate the energy harvesting figure of merit, $d_{33}g_{33}$. These were used to separate the effect of the piezoelectric properties from effects related to effective stiffness in the measured data.

Lastly, the stiffnesses of the samples were estimated from impedance spectroscopy data using the equation [40]:

$$Y = \frac{1}{s^E} = 4\rho_c f_r^{\,2} t_c^{\,2} \tag{17}$$

where f_a is the anti-resonance of the material and Y is the stiffness of the piezoelectric material in the direction of thickness. This formula was verified using materials with known mechanical properties before applying it to the new materials.

3. Results and discussion

3.1. Part 1: Beam stiffness tailoring study

The beams were excited with an acceleration of 1 g at the tip in a frequency range from 10 to 50 Hz (see Figures 5 and 6). To decrease the influence of dynamic effects, such as damping, connection or dynamics of shaker, etc. on the voltage response of the MFCs and to validate the model in COMSOL, the beams were excited from the free end of the beam in off-resonance conditions. Voltage responses were recorded under open-circuit conditions and compared to the results obtained from the COMSOL model. The results for different thicknesses of the beams agree well, see Figure 8. This step demonstrates that the modeling approach for MFC including the material properties used was suitable for application in the next stages of the study.

PZT-5A, PVDF, and MFCs bonded on beams made from different materials (acrylic, aluminum, steel) were then analyzed under the same boundary conditions (fixed one end, applied acceleration from the other end), whereby 1 g of tip

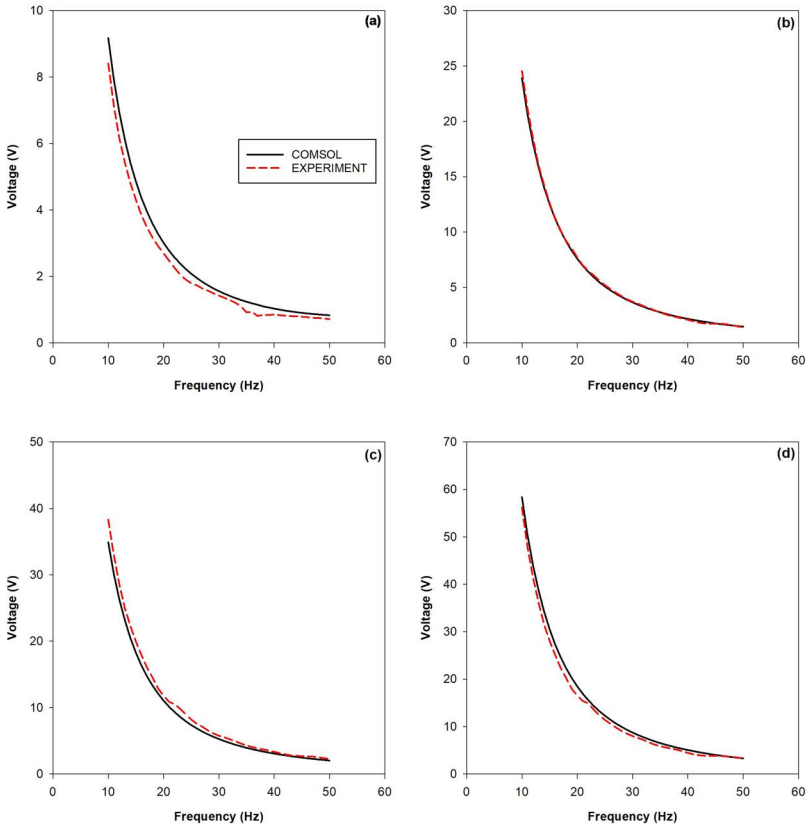

Figure 8. Voltage response of MFCs on the beams with thickness (ts) of (a) 0.25, (b) 0.5, (c) 0.7, and (d) 1.15 mm.

acceleration at 20 Hz was applied for a range of beam thicknesses. The dimensions and setup are shown in Figure 3. Here, the electrical energy transfer and electrical conversion efficiencies were kept constant using the same external circuit for all cases to ensure the changes in voltage response were solely due to mechanical energy transfer efficiency. The results obtained with COMSOL have been normalized by equating the maximum efficiency (i.e. the maximum power point) to 1 and adjusting the other values based on this ratio to clearly compare them to predicted results. The normalized efficiency results for different cases are shown in Figure 9. The energy transfer ratio increases with increasing stiffness of the beam until it reaches a maximum and then starts to decrease. This is the point where the beam can most effectively transfer its mechanical energy into the piezoelectric material. For the steel-PZT case, the effective stiffnesses (YI) of the beam and PZT patch match at $t_s = 0.33$ mm according to the prediction using Eq. (9). This agrees well with the maximum energy transfer condition predicted by the finite element model, which occurs at $t_s = 0.32$ mm. For the aluminum-PZT harvesters, the optimal thickness values were $t_s = 0.61$ mm and $t_s = 0.62$ mm from prediction and the finite element model, respectively. The optimum thickness increases for the aluminum-PZT configuration due to the lower elastic modulus of aluminum compared to steel. For the same dimensions of the beams and piezoelectric materials, the maximum energy transfer point increases with thickness as the elasticity of the beam decreases, as expected.

The study operates in the first vibration mode of the beams using applied accelerations at low frequencies.

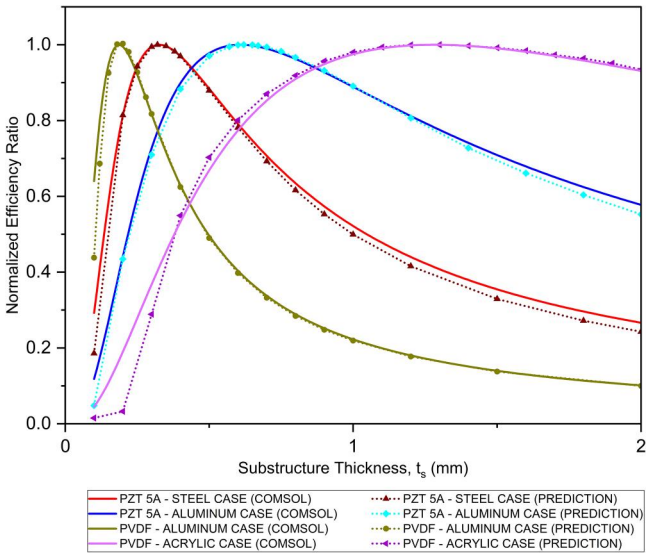

Figure 9. Mechanical energy transfer into PZT-5A and PVDF patches (normalized to 1) on different beams with respect to beam thickness modeled using COMSOL and predicted from Eq. (9).

Increasing the frequency activates additional vibration modes, which affects the voltage response. As the purpose of this study was to isolate the effect of mechanical impedance matching, the mode shape differences for different beams are not desirable. Figure 10 shows the normalized efficiencies for the case of MFC on different beam materials under different excitation frequencies. As mentioned previously, when the beams are excited in the first mode shape, the

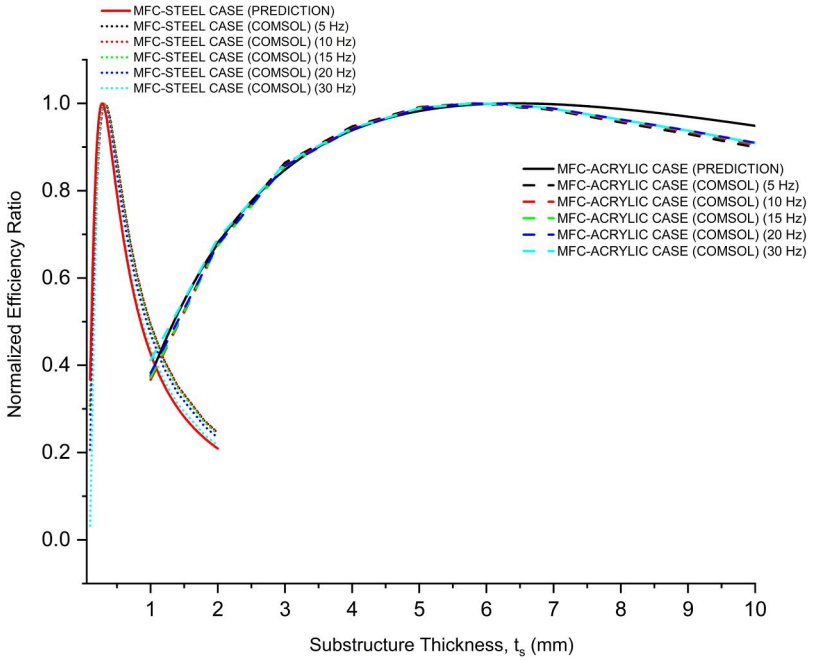

Figure 10. Mechanical energy transfer into MFC patches (normalized to 1) on different beams with respect to beam thickness modeled using COMSOL and predicted from Eq. (9).

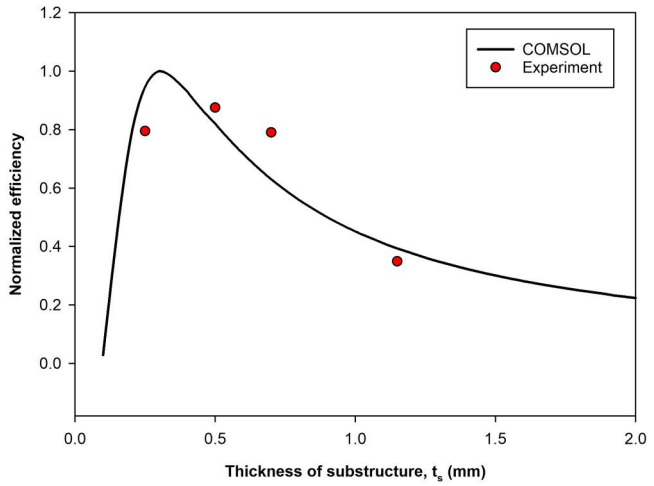

Figure 11. Comparison of mechanical energy transfer into MFC under 1 g (30 Hz) tip acceleration calculated by COMSOL and experiments.

change in the frequency does not affect the normalized efficiency and the point of maximum efficiency in terms of mechanical energy transfer. As vibration energy harvesters generally operate in the first mode, Eq. (9) can be used to predict the mechanical energy transfer efficiently in the applications.

Finally, the modeled data were compared to experimental data obtained from piezoelectric composite (MFC) patches on a steel beam with different thicknesses, see Figure 11. Experiments were made on four different thicknesses of the beam as described in Section 2.3. There is some deviation in the experiments compared to the analysis that is thought to arise from differences in the modeled piezoelectric to the real structure, in which the model does not consider the epoxy, encapsulation, or electrode stiffnesses. Small experimental errors are also expected due to the exact bonding location and amount of adhesive used when applying the piezoelectrics to the beam. The experimental data, however, follows a similar trend to the finite element simulation. The results have shown that mechanical energy transfer between materials is affected by the effective stiffnesses of the materials and energy transfer from substructure to the piezoelectric material can be improved by using materials with effective stiffnesses close to each other. For the bending mode of piezoelectric energy harvesting systems, mechanical energy transfer into piezoelectric materials can be predicted using a simple equation (Eq. 9), which can aid with the design of the supporting structure or the design of the piezoelectric material itself to improve the performance of an energy harvester.

3.2. Part 2: Piezocomposite stiffness tailoring study

Two piezoelectric composites with different epoxy/PZT ratios with the same dimensions were fabricated and are referred to herein as PZT-1 and PZT-2. Figure 12 shows SEM images of the microstructures of the two freeze cast composites taken such that the freezing direction was vertical. The high-density ceramic regions appear in bright contrast whereas the low-density epoxy appears darker in the SEM images taken in backscattered electron detection mode. Freeze casting was used to create highly aligned porous ceramic microstructures, with pores aligned along the temperature gradient during freezing, however, PZT-1 had poor microstructural alignment whereas PZT-2 contained highly aligned pores. However, the piezoelectric properties of both PZT-1 and PZT-2 were high (~90% of the manufacturer value for the dense PZT NCE55) and the difference in porosity and stiffness made them suitable for further experiments. The material properties of the piezoelectric composites are shown in Table 3 with the properties of dense

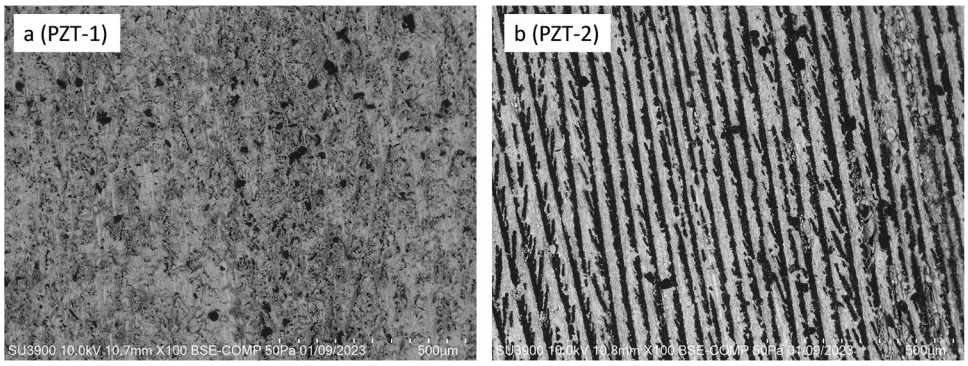

Figure 12. Scanning electron micrograph of the (a) PZT-1 and (b) PZT-2 freeze casted composites.

Table 3. Material properties of the freeze cast piezoelectric composites.

	PZT-1	PZT-2	NCE55
Piezoelectric charge coefficient, d_{33}, pC/N	580	577	670
Relative permittivity, $\varepsilon_{33}^T/\varepsilon_0$	2320	2672	5000
Piezoelectric voltage coefficient, g_{33}, Vm/N	0.0282	0.0244	0.019
PZT volume fraction	0.58	0.73	1.00
Stiffness, Y_{33}, GPa	24	39	60

NCE55 where the values are taken from literature [41]. It can be seen that the piezoelectric charge coefficient of PZT-1 and PZT-2 are slightly lower than dense NCE55, however, the relative permittivity of piezoelectric composites is nearly half of the dense material, which results in a high piezoelectric voltage coefficient, g_{33}. As different solid loadings were used in the freeze cast suspensions to fabricate PZT-1 and PZT-2, they have different porosities (42 and 27 vol.%, respectively). This results in a lower stiffness (~25 GPa), estimated from impedance data and Eq. (17), compared to PZT-2 (39 GPa).

Low stiffness acrylic beams ($Y = 3.2$ GPa) with dimensions of $80 \times 30 \times 3\,\text{mm}^3$ were used as a substructure and the piezoelectric composites were bonded on these beams as shown in Figure 13. The notation of axis system is rotated to account for the different polarization directions (parallel to z-axis) for the freeze cast composites compared to the MFC composite study schematically represented in Figure 13. The energy harvesting performances were tested using the same experimental setup described in Section 2.3, however, one end of the beam was connected from one point to the shaker and the other end was kept free as shown in Figure 14. The beam was accelerated in a frequency range from 100 to 180 Hz by the shaker from the base excitation and the voltage response of the piezoelectric composites was measured.

The open circuit voltage of the piezoelectric material can be calculated from:

$$V_{oc} = \frac{d_{33}}{\varepsilon_{33}^T}\sigma_3 t_c = g_{33}(Y_{33}S_3)t_c \tag{18}$$

where σ_3 is the stress and S_3 is the strain applied on the piezoelectric material in the direction of polarization. This equation assumes a linear relationship between the applied stress, σ_3, and the strain, S_3, linked by the stiffness of the material, Y_{33}. We have used a single value for stiffness rather than the constant electric field (short circuit) term usually used in piezoelectric literature, c_{33}^E, to simplify the

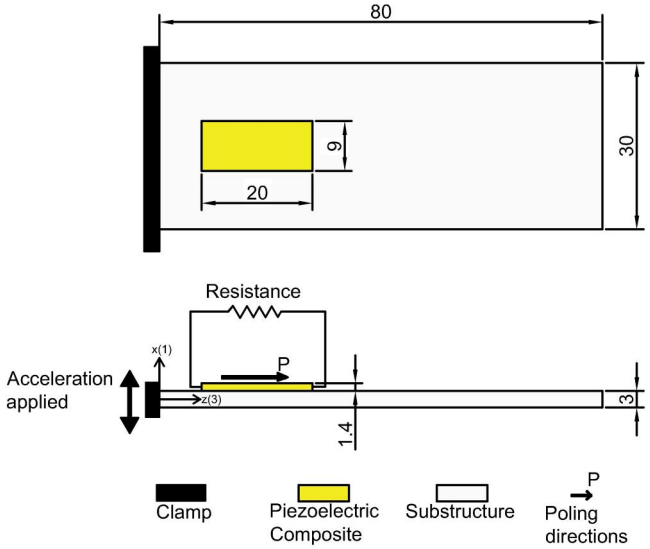

Figure 13. Dimensions of acrylic beam and piezoelectric composites (all units in mm).

analysis. The output voltage is proportional to the piezoelectric voltage coefficient, $g_{33} = d_{33}/\varepsilon_{33}^T$. The open circuit voltage is obtained when no charge can flow between electrodes which is in the case of an infinite external load is applied to the circuit. The longitudinal piezoelectric charge coefficient, d_{33}, was used as the piezoelectric material was polarized in the direction of strain applied. As the aim of this study was to investigate the effect of the effective stiffness on the voltage response, the other terms in the equation are eliminated by accounting for the variations in the measured piezoelectric, dielectric, and mechanical properties of the freeze cast samples. The electromechanical conversion ratio of the piezoelectric materials was normalized according to the piezoelectric voltage coefficients, g_{33}, of PZT-1 and PZT-2. For this, the voltage response of PZT-2 was multiplied by the ratio of voltage constants of PZT-1 and PZT-2 as given below,

$$V_{norm,2} = V_{oc,2}\frac{g_{33,1}}{g_{33,2}} = \ 1.15(V_{oc,2}) \tag{19}$$

where $V_{norm,2}$ is the normalized voltage of PZT-2, $g_{33,1}$ is voltage constant of PZT-1 and $g_{33,2}$ is the voltage constant of PZT-2. By using the normalization constant, the effect of electromechanical conversion efficiency on total efficiency

was eliminated. This leaves stress as the only variable to affect the normalized voltage, which depends on the energy transfer ratio and elasticity of the material as discussed in Section 2. The normalized and unnormalized voltage responses of piezoelectric composites for the same applied mechanical energy are shown in Figure 15.

The PZT composites were bonded onto an acrylic beam which was less stiff than the PZT composites. Increasing the porosity/epoxy volume fraction decreased the stiffness of the composites, which enhanced the stiffness matching between beam and piezoelectric material and thereby increased the strain energy transfer to the piezoelectric material. There is an increase in voltage response as seen in Figure 15, however, there is not a significant change in normalized voltage response. The effective stiffness ratios of PZT-1 and PZT-2 to the substructure (K_1/K_2) are 0.68 and 0.51, respectively. Therefore, the energy transfer ratio of 96 and 89% is expected, respectively for PZT-1 and PZT-2. This agrees with the 8% increase in the voltage response which results in a 16% increase in power gain from PZT-1 compared to PZT-2 once the data are normalized with respect to the g_{33}-coefficient (Figure 15(a)). Although there may be other factors that affect the results here and there is not a power gain in the frequencies rather than resonance frequency between two cases, this can be a starting point for future studies as this paper gives a proof-of-concept idea for controlling the mechanical properties of piezoelectric materials using fabrication methods, such as freeze casting that offer relatively simple control over piezoelectric ceramic volume fraction and microstructure.

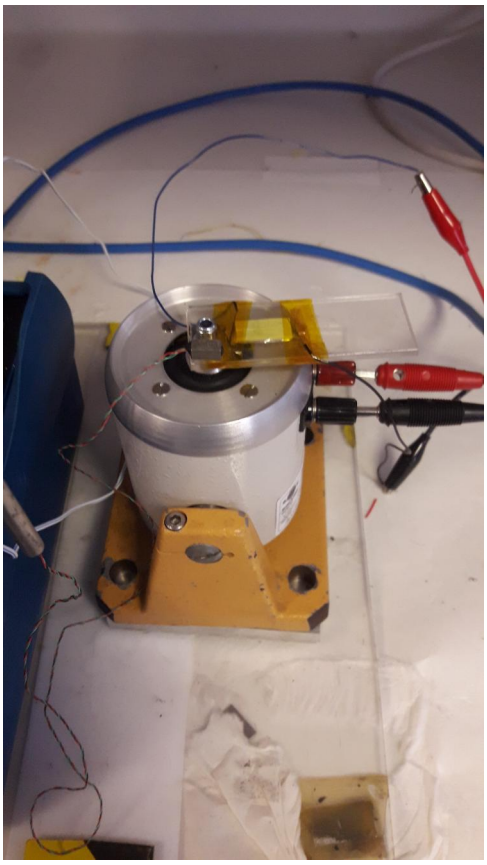

Figure 14. Piezocomposites bonded on beam and attached to shaker and measurement system.

4. Conclusion

In this work, we investigated the importance of effective stiffness matching between the active piezoelectric component and the substructure through which mechanical energy is supplied as a method to increase piezoelectric energy harvesting performance. There are many parameters that affect the energy harvesting from piezoelectric materials and mechanical energy transfer is one of the most important points in this process. Effects, such as mechanical to electrical conversion rate and piezoelectric harvesting figure of merits were accounted for here to isolate the effect of mechanical energy transfer between materials. The results have shown that the energy transfer rate between the materials can be optimized by matching the effective stiffnesses of the materials. For the same mechanical energy input into the substructure, mechanical energy transfer into piezoelectric material dropped by 10% for an effective stiffness ratio of 0.5, and reduced to 35% of the optimal value for an effective stiffness ratio of 0.25; this was further decreased at lower stiffness ratios. This agreed well with our analytical prediction based on strain energy transfer between a cantilever beam and piezoelectric material due to the relative effective stiffness terms of each component. Finite element analysis and experimental studies were used to validate the results,

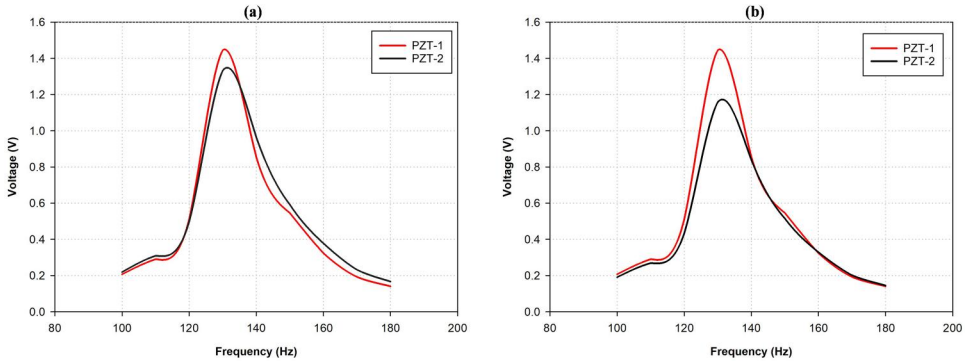

Figure 15. Voltage responses of the PZT composites under same mechanical energy input (a) normalized for piezoelectric voltage constant (b) without normalization (Eq. 19).

which resulted in a simple method of tuning the material (Young's modulus, Y) and structural (second moment of area, I) properties of both the beam and the piezoelectric patch was shown to be an effective method of improving energy harvesting output.

In the second part of the study, the freeze casting method was used to produce porous piezoceramics that were infiltrated with epoxy to fabricate piezocomposites. The effective stiffnesses of the piezocomposites were controlled by changing the volume fraction of ceramic and the epoxy used to match with the substructure used in the study. After the piezoelectric and dielectric properties were corrected, the power response was increased by 16% using piezoelectric composites with a mechanical stiffness better matched to the substrate, despite them having similar voltage and energy harvesting figures of merit.

This study has demonstrated the importance of effective stiffness matching on energy transfer efficiency for piezoelectric energy harvesters and offers a simple formula to predict how mechanical impedance matching can be considered in the early design of an energy harvester. The freeze casting method is proposed as an approach to produce piezoelectric composites with good piezoelectric properties and mechanical properties that can be easily adjusted to maximize the power output of a piezoelectric energy harvester.

Disclosure statement

No potential conflict of interest was reported by the author(s).

Funding

James I. Roscow and Bastola Narayan thank the EPSRC for financial support (Grant No: EP/V011332/1). Polat Kurt thanks the TUBITAK for fellowship during the research (1059B142000359).

ORCID

James I. Roscow http://orcid.org/0000-0003-1652-5058

Data availability statement

All data that support the findings of this study are included within the article and in Supplementary Information.

References

[1] A. Toprak and O. Tigli, Piezoelectric energy harvesting: state-of-the-art and challenges, Appl. Phys. Rev., vol. 1, no. 3, pp. 031104, 2014. DOI: 10.1063/1.4896166.

[2] T. Li and P.S. Lee, Piezoelectric energy harvesting technology: from materials, structures, to applications, Small Struct., vol. 3, no. 3, pp. 2100128, 2022. DOI: 10.1002/sstr.202100128.

[3] H. Kim, S. Priya, H. Stephanou, and K. Uchino, Consideration of impedance matching techniques for efficient piezoelectric energy harvesting, IEEE Trans. Ultrason. Ferroelectr. Freq. Control., vol. 54, no. 9, pp. 1851–1859, 2007. DOI: 10.1109/tuffc.2007.469.

[4] J.I. Roscow, H. Pearce, H. Khanbareh, S. Kar-Narayan, and C.R. Bowen, Modified energy harvesting figures of merit for stress- and strain-driven piezoelectric systems, Eur. Phys. J. Spec. Top., vol. 228, no. 7, pp. 1537–1554, 2019. DOI: 10.1140/epjst/e2019-800143-7.

[5] D. Man, Y. Zhang, G. Xu, X. Kuang, H. Xu, L. Tang, and T. Han, Improving energy harvesting from low-frequency excitations by a hybrid tri-stable piezoelectric energy harvester, Alexandr. Eng. J., vol. 76, pp. 153–165, 2023. DOI: 10.1016/j.aej.2023.06.031.

[6] M. Ravanbod and S. Ebrahimi-Nejad, Perforated auxetic honeycomb booster with reentrant chirality: a new design for high-efficiency piezoelectric energy harvesting, Mech. Adv. Mater. Struct., pp. 1–16, 2023. DOI: 10.1080/15376494.2023.2280997.

[7] S. Sadikbasha, B. Radhika, and V. Pandurangan, Auxetic hexachiral cantilever beams for piezoelectric vibration energy harvesting, Smart Mater. Struct., vol. 31, no. 10, pp. 105015, 2022. DOI: 10.1088/1361-665X/ac8d3e.

[8] A.R.G. da Silveira and G.B. Daniel, Optimization analysis of an energy harvester for smart tilting pad journal bearings considering higher vibration modes, Mech. Syst. Sig. Process., vol. 166, pp. 108404, 2022. DOI: 10.1016/j.ymssp.2021.108404.

[9] S. Bouhedma, S. Hu, A. Schütz, F. Lange, T. Bechtold, M. Ouali, and D. Hohlfeld, Analysis and characterization of optimized dual-frequency vibration energy harvesters for low-power industrial applications, Micromachines, vol. 13, no. 7, pp. 1078, 2022. DOI: 10.3390/mi13071078.

[10] K. Chadha, V. Mahesh, A.S. Mangalasseri, and V. Mahesh, On analysing vibration energy harvester with auxetic core and magneto-electro-elastic facings, Thin. Walled Struct., vol. 184, pp. 110533, 2023. DOI: 10.1016/j.tws.2023.110533.

[11] H. Yu, C. Hou, X. Shan, X. Zhang, H. Song, X. Zhang, and T. Xie, A novel seesaw-like piezoelectric energy harvester for low frequency vibration, Energy, vol. 261, pp. 125241, 2022. DOI: 10.1016/j.energy.2022.125241.

[12] M. Askari, E. Brusa, and C. Delprete, Design and modeling of a novel multi-beam piezoelectric smart structure for vibration energy harvesting, Mech. Adv. Mater. Struct., vol. 29, no. 28, pp. 7519–7541, 2022. DOI: 10.1080/15376494.2021.2001122.

[13] S.S. Raju, M. Umapathy, and G. Uma, Design and analysis of high output piezoelectric energy harvester using non uniform beam, Mech. Adv. Mater. Struct., vol. 27, no. 3, pp. 218–227, 2020. DOI: 10.1080/15376494.2018.1472341.

[14] V.T. Rathod, A review of electric impedance matching techniques for piezoelectric sensors, actuators and transducers, Electronics, vol. 8, no. 2, pp. 169, 2019. DOI: 10.3390/electronics8020169.

[15] N.A. Kong, D.S. Ha, A. Erturk, and D.J. Inman, Resistive impedance matching circuit for piezoelectric energy harvesting, J. Intell. Mater. Syst. Struct., vol. 21, no. 13, pp. 1293–1302, 2010. DOI: 10.1177/1045389X09357971.

[16] H. Jabbar, H.J. Jung, N. Chen, D.H. Cho, and T.H. Sung, Piezoelectric energy harvester impedance matching using a piezoelectric transformer, Sens. Actuators A, vol. 264, pp. 141–150, 2017. DOI: 10.1016/j.sna.2017.07.036.

[17] B. Zhao and J. Liang, On the circuit solutions towards broadband and high-capability piezoelectric energy harvesting systems, Active and Passive Smart Structures and Integrated Systems XII, vol. 10595, pp. 71–78, SPIE, 2018. DOI: 10.1117/12.2296333.

[18] M. Bonnin, F.L. Traversa, and F. Bonani, An impedance matching solution to increase the harvested power and efficiency of nonlinear piezoelectric energy harvesters, Energies, vol. 15, no. 8, pp. 2764, 2022. DOI: 10.3390/en15082764.

[19] Z. Yang, A. Erturk, and J. Zu, On the efficiency of piezoelectric energy harvesters, Extreme Mech. Lett., vol. 15, pp. 26–37, 2017. DOI: 10.1016/j.eml.2017.05.002.

[20] M. Kim, J. Dugundji, and B.L. Wardle, Efficiency of piezoelectric mechanical vibration energy harvesting, Smart Mater. Struct., vol. 24, no. 5, pp. 055006, 2015. DOI: 10.1088/0964-1726/24/5/055006.

[21] Y.-C. Shu and I.C. Lien, Efficiency of energy conversion for a piezoelectric power harvesting system, J. Micromech. Microeng.,

vol. 16, no. 11, pp. 2429–2438, 2006. DOI: 10.1088/0960-1317/16/11/026.
[22] K. Uchino, Piezoelectric energy harvesting systems – essentials to successful developments, Energy Tech., vol. 6, no. 5, pp. 829–848, 2018. DOI: 10.1002/ente.201700785.
[23] K. Uchino, Essentials of Piezoelectric Energy Harvesting, World Scientific, Singapore, 2021.
[24] S. Raghavan, A. Sharma, and R. Gupta, Resonant frequency tuning of a novel piezoelectric vibration energy harvester (PVEH), Mech. Adv. Mater. Struct., pp. 1–16, 2023. DOI: 10.1080/15376494.2023.2209078.
[25] W. Wilkie, NASA MFC piezocomposites: a development history, Proceedings of the International Symposium on Macro Fiber Composite Applications ISMA, Volkswagen "Transparent Factory", pp. 27–28, Dresden, Germany, 2005.
[26] T.P. Daue, J. Kunzmann, and A. Schönecker, 2008. Energy harvesting systems using piezo-electric macro fiber composites, IEEE International Symposium on Electrets (ISE13), Paper, vol. 27.
[27] M. Mallouli and M. Chouchane, Piezoelectric energy harvesting using macro fiber composite patches, Proc. Inst. Mech. Eng. Part C J. Mech. Eng. Sci., vol. 234, no. 21, pp. 4331–4349, 2020. DOI: 10.1177/0954406220920321.
[28] Y. Zhang, J. Roscow, M. Xie, and C. Bowen, High piezoelectric sensitivity and hydrostatic figures of merit in unidirectional porous ferroelectric ceramics fabricated by freeze casting, J. Eur. Ceram. Soc., vol. 38, no. 12, pp. 4203–4211, 2018. DOI: 10.1016/j.jeurceramsoc.2018.04.067.
[29] J.I. Roscow, Y. Zhang, M.J. Kraśny, R.W.C. Lewis, J. Taylor, and C.R. Bowen, Freeze cast porous barium titanate for enhanced piezoelectric energy harvesting, J. Phys. D Appl. Phys., vol. 51, no. 22, pp. 225301, 2018. DOI: 10.1088/1361-6463/aabc81.
[30] J.I. Roscow, Y. Li, and D.A. Hall, Residual stress and domain switching in freeze cast porous barium titanate, J. Eur. Ceram. Soc., vol. 42, no. 4, pp. 1434–1444, 2022. DOI: 10.1016/j.jeurceramsoc.2021.11.046.
[31] T. Fuchigami, Y. Sumiya, and K.I. Kakimoto, Ferroelectric domain formation and photocatalytic activity on porous alkali niobate piezoelectric ceramics, J. Ceram. Soc. Jpn., vol. 129, no. 7, pp. 425–431, 2021. DOI: 10.2109/jcersj2.21052.
[32] L. Wang, L. Zhao, Z. Jiang, G. Luo, P. Yang, X. Han, X. Li, and R. Maeda, High accuracy comsol simulation method of bimorph cantilever for piezoelectric vibration energy harvesting, AIP Adv., vol. 9, no. 9, pp. 1–9, 2019. DOI: 10.1063/1.5119328.
[33] Available from https://info.piezo.com/hubfs/Data-Sheets/piezo-material-properties-data-sheet-20201112.pdf
[34] R. Mahidhar, K. Prakash, R.N. Aswathi, M.V.N. Prasad, and S. Sambandan, Vibration spectrum analyzer using stretched membranes of polymer piezoelectrics for sensor networks, Meas. Sci. Technol., vol. 24, no. 5, pp. 055108, 2013. DOI: 10.1088/0957-0233/24/5/055108.
[35] Z. Dong, C. Faria, M. Hromčík, B. Pluymers, M. Šebek, and W. Desmet, Equivalent force modeling of macro fiber composite actuators integrated into non-homogeneous composite plates for dynamic applications, Smart Mater. Struct., vol. 26, no. 9, pp. 095040, 2017. DOI: 10.1088/1361-665X/aa7bd0.
[36] S.Q. Zhang, Y.X. Li, and R. Schmidt, Modeling and simulation of macro-fiber composite layered smart structures, Compos. Struct., vol. 126, pp. 89–100, 2015. DOI: 10.1016/j.compstruct.2015.02.051.
[37] Y. Kuang, and M. Zhu, Evaluation and validation of equivalent properties of macro fibre composites for piezoelectric transducer modelling, Compos. Part B Eng., vol. 158, pp. 189–197, 2019. DOI: 10.1016/j.compositesb.2018.09.068.
[38] Available from https://www.smart-material.com/MFC-product-P2V2.html
[39] A. Deraemaeker, H. Nasser, A. Benjeddou, and A. Preumont, Mixing rules for the piezoelectric properties of macro fiber composites, J. Intell. Mater. Syst. Struct., vol. 20, no. 12, pp. 1475–1482, 2009. DOI: 10.1177/1045389X09335615.
[40] B. Jaffe, W. Cook, and H. Jaffe, Piezoelectric Ceramics, Academic, London, vol. 3, 1971.
[41] Available from https://seacorpiezo.com/material-specifications/lead-zirconate-titanate-soft/nce-55/